Journal of the Korea Institute of Applied Superconductivity and Cryogenics
Vol.7, No.2, (2005), pp.1~6

Observing Thermal Counterflow in He II by the Particle Image Velocimetry Technique

S. W. Van Sciver

National High Magnetic Field Laboratory
FAMU-FSU College of Engineering
Tallahassee, FL 32310, USA

vnsciver@magnet.fsu.edu

Abstract-- **The Particle Image Velocimetry (PIV) technique can be used to obtain a whole-field view of thermal counterflow velocity profile in He II. Using commercially available microspheres, we have been able to visualize the normal fluid velocity in He II thermal counterflow; however, the measured velocities are less than predicted from the two fluid model. None the less, the PIV is a useful tool for observing the counterflow field in He II flow, particularly where the flow is complex as occurs through channel constrictions or around bluff objects. The present paper shows recent results using PIV to observe He II counterflow. Two cases are discussed: 1D channel flow and turbulent flow around a circular cylinder.**

1. INTRODUCTION

In the two-fluid model, He II is thought to be composed of two interpenetrating components: normal fluid and superfluid. When there is a heat source deposited in He II, the normal fluid flows away from the heat source carrying the entropy while and the superfluid moves towards the heat source conserving mass and momentum. This kind of internal convection process is termed "thermal counterflow" and leads to heat transfer which is much more effective than ordinary thermal conduction or classical convection. Thermal counterflow, as one of the most interesting and fundamental processes in He II research, has been studied extensively [1]; however, there are still many questions left unanswered about the process, such as how the two fluid components interact with each other, and how this interaction will affect the development of turbulence in the inviscid superfluid component. Also, due to the many technical applications for He II, an understanding of the heat transport in this unique fluid is vital to advancing the technology.

In most of the previous studies of He II thermal counterflow, the temperature and pressure gradients are measured, while the velocity fields of the normal and superfluid components are only inferred from analysis. Researchers have used a number of techniques in an attempt to visualize the two fluid component velocities; however since they are not directly observable, all methods rely on seeding the flow with objects that can be seen and presumably follow the fluid components. Examples of seeding particles include hollow glass spheres, solid polymer micro-spheres, solid H_2/D_2 particles and He^3 drops [2-3]. For some experiments in which the particle velocity was actually measured, only point measurements were conducted using the Laser Doppler velocimetry (LDV) technique [4-5].

To explore some of these questions, detailed fluid dynamics measurements of the entire velocity field in thermal counterflow are required. To obtain such data, it is necessary to utilize innovative visualization techniques.

The present article summarizes our recent developments in the study of counterflow in He II using the Particle Image Velocimetry (PIV) technique. PIV is a powerful fluid dynamics tool that allows the entire flow field to be visualized. The article begins with a summary of the two fluid model for He II, which is necessary to understanding the basis for the interaction between the seeding particles and the He II. Next is a brief discussion of the techniques used to seed particles in He II and measure counterflow. Results and discussion summarizes three cases of interest. First, measurement of the normal fluid velocity during steady heat transport in a one dimensional channel is considered. Results are compared to the predictions of the two fluid model. Second, transient heat transport in He II is observed using the same techniques. The final topic is the observed counterflow velocity field that occurs during heat transport around a cylinder. The implications these results have on the modeling of heat transport in He II are discussed.

2. BACKGROUND OF SUPERFLUID HELIUM

One of the exceptional characteristics of liquid helium is that it can exist in either of two different phases, normal helium (or He I) and superfluid helium (or He II). These two phases are separated by a so-called lambda transition, which under saturated pressure is about 2.2 K. While He I is essentially a Navier-Stokes fluid that obeys the hydrodynamics described by the classical fluid dynamics equations, He II displays many unique transport properties, such as a superior thermal conductivity that is many orders

of magnitude greater than that of ordinary fluids, and a lowest kinematic viscosity of all known fluids, about three orders of magnitude smaller than that of air [6]. These unique transport properties of He II can be interpreted in terms of a two-fluid model [7]. According to this model, He II is comprised of two interpenetrating fluid components: normal fluid and superfluid. The normal fluid component behaves like an ordinary Navier-Stokes fluid with a density ρ_n, viscosity η_n, and specific entropy s_n. In contrast, the superfluid has a density ρ_s, but no viscosity and entropy, i.e. $\eta_s = 0$ and $s_s = 0$. Also, each fluid component has its own independent velocity field, $\vec{v}_n$ and $\vec{v}_s$ respectively.

Assuming that a certain heat flux q is applied to He II, since only the normal fluid component has the entropy, it will carry the heat away from the source. At the same time, the superfluid component will move in the opposite direction in order to conserve the mass. Thus, a relative motion between the normal fluid and superfluid, termed thermal counterflow, is established. As indicated, there is a "zero net mass (ZNM) flow" condition for thermal counterflow in static He II, which is quantitatively described by setting the total fluid momentum equal to zero,

$$\rho_n \vec{v}_n + \rho_s \vec{v}_s = 0 \tag{1}$$

Since all the applied heat is carried by the normal fluid, the averaged normal fluid velocity is

$$\bar{v}_n = \frac{q}{\rho s T} \tag{2}$$

where $\rho = \rho_n + \rho_s$ is the bulk density of He II, $s = s_n$ is the total entropy, and T is the absolute temperature. From the above two equations, the averaged relative velocity between the normal fluid and superfluid can be simply written as

$$\bar{v}_r = \left|\bar{v}_n - \bar{v}_s\right| = \frac{q}{\rho_s s T} \tag{3}$$

When the applied heat flux q is increased so that the relative velocity is greater than a critical value, quantum turbulence is generated in the superfluid component, resulting in a mutual friction force between the normal fluid and superfluid.

This mutual friction force causes a non-linear temperature gradient to be established in the He II which leads to conduction-like heat transport. In this regime, the thermal gradient is governed by the following relation,

$$q = -\left(f^{-1} \frac{dT}{dx} \right)^{1/3} \tag{4}$$

where f^1 is the He II thermal conduction function [6]. In transient heat transport, this mechanism leads to a diffusion like transport in the He II.

The mutual friction process is the mechanism that is the most important thermal transport mechanism for large scale He II applications. It has been successful at describing the results from a large number of experiments as well as the design He II heat exchangers [8] and the theory of magnet stability in He II [9].

3. EXPERIMENTAL SETUP AND PROCEDURE

To conduct a PIV experiment in He II, one needs an optical cryostat together with a complete PIV measurement apparatus including a CCD camera, a dual head laser, beam expanding optics, synchronizer for timing and triggering laser and camera, and a computer for data acquisition. More details about the experimental setup used in the present experiments and how to operate the PIV apparatus can be found in reference [10].

The test section of the present set of experiments, shown in Fig. 1, is a rectangular thermal counterflow channel immersed inside He II bath. It is 200 mm long with a 38.75×19.5 mm^2 cross-section and is made of 6.4 mm thick G-10 plate to reduce heat loss through the walls. The top end of the channel is open to the helium bath while the lower end is closed. On each side wall of the channel there is an optical windows for the laser sheet in and out. The front wall, a 45×20 mm^2 optical window, is used for the CCD camera to capture images. Thermal counterflow is generated by a thin film heater (47.7 nm) made of Nichrome (80% Ni and 20% Cr), having a thermal time constant around 10 ns and essentially uniform heat flux.

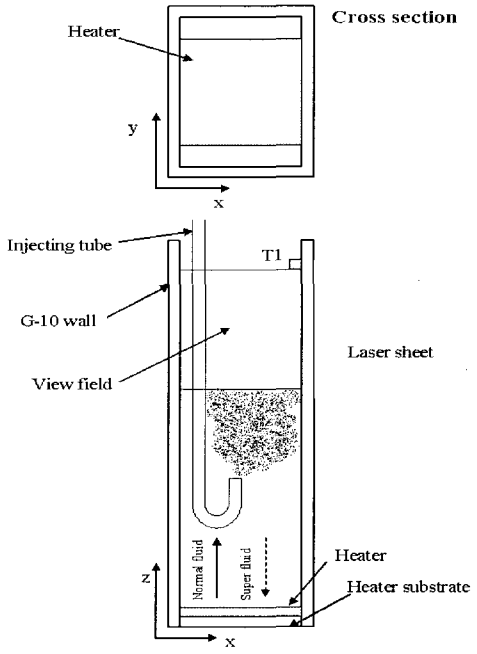

Fig. 1. Schematic of PIV counterflow channel used in the present experiments (T1 is a thermometer).

The particle selection and seeding for He II experiments is critical to making a successful measurement. It is best to have particles that are neutral density and less than 10 m in diameter with a narrow size distribution. However, since He II has a very low density (S.G. = 0.145), it is difficult to meet the density requirements. Thus, for most of the experiments described herein, we have used polymer microspheres of diameter 1.7 m, and S.G. = 1.1. Minor corrections to the data are required for gravitational force on the particles.

To inject particles into the channel, a thin copper tube is connected to the seeding apparatus and placed inside the channel. The injection position is about 100 mm below the optical port of the channel. Before starting the experiment, the polymer tracer particles are carefully purged following the procedures described in reference [2] in preparation for injecting. With the liquid helium in the superfluid state at a certain bath temperature, the tracer particles are injected into the channel using the pressure difference between helium gas source and liquid helium. After the particles enter the flow field, the normal fluid carries them upward. When passing through the optical port, the particles are illuminated by laser sheet, and their images are recorded by the CCD camera and stored for PIV analysis.

4. RESULTS AND DISCUSSION

4.1. Steady state 1D thermal counterflow

With the liquid helium bath controlled at a constant temperature and the tracer particles in the counterflow channel, the heater is turned, which drives the tracer particles along in the direction of normal fluid velocity (away from the heater). For steady state measurements, the CCD camera is operated at a frequency of 5 Hz to achieve highest resolution. During each data acquisition process, a number of pairs of images are collected within a time interval of the experiment and, for each pair of images, a cross-correlation algorithm applied to determine the displacement of particles. In the present experiments, an interrogation window of 48 × 48 pixels (one pixel is 6.7 μm square) is used. A total of 400 (20 × 20) vectors of velocity can be calculated by the PIV analysis software with a spatial resolution of around 1 mm, making it possible to study the details of velocity field. In order to obtain a stable PIV result, the multiple pairs of images can be further averaged to generate the final velocity profile of normal fluid.

As shown in Fig 2, the direction of particle motion uniformly upward (away from the heater) with the horizontal component of velocity being close to zero. Also note that the velocity is uniform across the flow field suggesting that any thermal boundary layer must be much thinner than the resolution of the measurement (about 1 mm). The magnitude of vertical velocity, however, is not quiet uniform with a variation from 40 to 45 mm/s, resulting from the inhomogeneity of particle concentration and insufficient image pairs to be averaged. Also, note that the computed normal fluid velocity based on Eq. 2 is about 100 mm/s indicating that the particles are moving at roughly half the theoretical normal fluid velocity, v_n.

Fig. 3 compares the measured particle velocity, v_p, to v_n for all temperatures and heat fluxes. These data indicate that the relative factor of two between measured and computed velocity appears to by independent of bath temperature. It is not clear what exactly causes the discrepancy between the particle velocities and v_n. However, some hints have been given by previous researchers. Donnelly et al [11] suggested that the response of tracer particles to the normal fluid velocity field is generally complicated due to the presence of two velocity fields in He II and quantized vortex lines in superfluid component, which can trap the tracer particles and affect their movement. Experimental evidence for this suggestion has been reported by Chung and Critchlow, who measured the motion of suspended particles in pure superfluid flow and observed that the particles track the superfluid velocity field even though the superfluid component is inviscid [12]. An argument can be made that the superfluid component may exert an additional force on the tracer particles in He II. This force, which would be in the opposite direction to the viscous drag force from normal fluid component, would slow down the particle velocity relative to v_n. Thus, any theory designed to predict the motion of the particles in He II counterflow should include this mechanism [13].

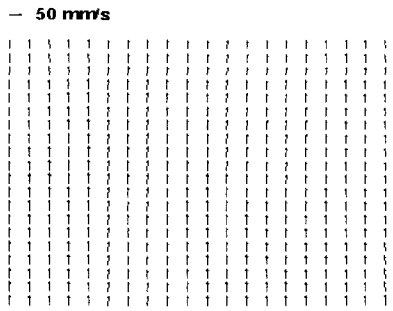

Fig. 2. PIV results for counterflow (T=1.62 K, q= 7.24 kW/m^2).

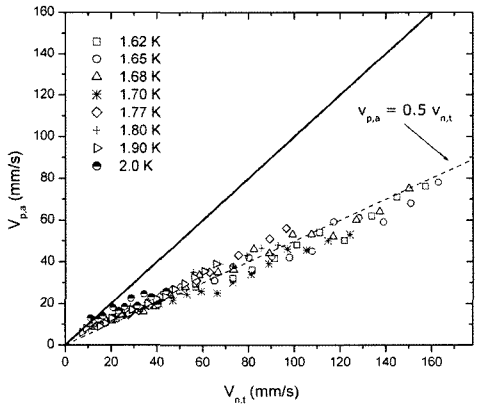

Fig. 3. Measured particle velocity versus the computed normal fluid velocity for all temperatures and heat fluxes.

4.2. Transient 1D thermal counterflow

PIV can also be used to study transient heat transport in He II. There are two principal mechanisms that control time varying heat transport in He II. For very short duration heat pulses, the heat or entropy is carried by a thermal wave called "second sound" that propagates at approximately 20 m/s. This process is associated with ideal superfluid and does not depend on the existence of turbulence in the superfluid component. Second sound is a unique mechanism in He II and is associated with fluctuations in the relative density of the two fluid components in the fluid. However, there are physical limits to the total heat transport by this mechanism above which turbulence is established in the superfluid component [14]. The existence of turbulence in the superfluid component causes attenuation of the second sound. Beyond that, the transient heat transport is governed by thermal diffusion in the turbulent state [15].

It is of interest to study the propagation of second sound and thermal diffusion in He II using PIV [16]. These experiments are performed in a similar fashion to the steady state experiments except that the transient particle motion must be measured with a high-speed CCD camera. Also, because this is a transient measurement, it is not possible to average the data to reduce noise. A typical measurement consists of a square heat pulse of a given amplitude and duration. The particle motion is then monitored versus time following the initiation of the heat pulse.

Fig. 4 shows a typical trace of particle velocity for a 1 second long pulse of amplitude 11.2 kW/m^2 at 1.61 K. The leading edge of the pulse arrives in the view field at a time corresponding to the transit of second sound, $t = H/c_2 = 7.5$ ms, where H is the distance from the heater and the view field. On arrival of the second sound pulse, the particle velocity reaches a steady value for approximately 6 ms, after which it starts to drop. Again, the peak velocity is less than that of the normal fluid component again suggesting

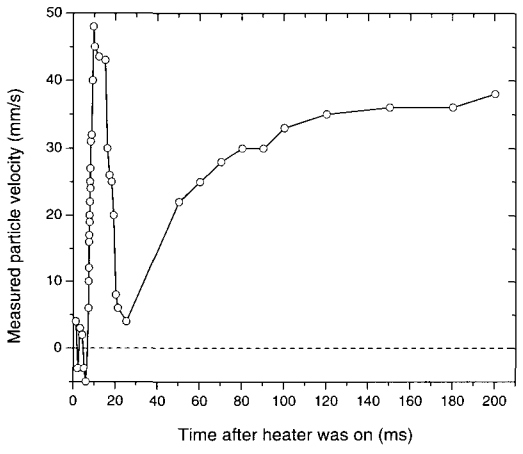

Fig. 4. The particle velocity profile induced by a 1 second long heat pulse with applied heat flux of 11.2 kW/m2. The bath temperature is 1.61 K.

the particles may be affected by the superfluid component. The finite extent of the second sound pulse can be explained by the theory of critical energy flux in second sound shock. Accordingly, when the applied energy flux exceeds a critical value, high intensity superfluid turbulence is formed behind the pulse, preventing further heat transport by second sound [15]. Above this critical energy flux, the excess energy that cannot be transported by second sound forms a thermal boundary layer adjacent to the heater and is then transported in diffusion. This process has also been confirmed by the measured velocity profile shown in Fig. 4, where the heat diffusion is represented by the second particle velocity rise (the first one is induced by second sound). Compared with second sound, the development of heat diffusion is much slower, and it may take hundreds of milliseconds to reach steady state.

4.3. Steady state thermal counterflow around a cylinder

Most investigations of heat transport in He II have focused on one dimensional channel geometry where the component velocities do not change rapidly in space and gradients are in one dimension. However, there are a number of important technical applications for He II, where the heat flow is more complex warranting investigations of non-linear geometry. Examples of more complex geometries that have been studied include radial heat flow from a cylinder [17] or flow through orifices [18-19].

We have used the PIV technique to investigate the heat transport process in He II around a cylinder. In this case, a right circular transparent glass cylinder of 6.35 mm OD was placed in the view field of the same counterflow channel. In the widest part of the cylinder, the channel cross section was reduced to 68% of its original value. With this cylinder in place, steady state counterflow heat transport was applied as discussed above measuring the particle velocity in the vicinity of the cylinder. Examples of these results are shown in Fig. 5 for two cases: a) heat flux of 4 kW/m^2 at a bath temperature of 1.6 K and b) heat flux of 11.2 kW/m^2 at a bath temperature of 2.03 K. Comparing these two cases indicates a higher level of turbulence for case b) with several large scale vorticies present.

For classical flow around a cylinder, vortex shedding leads to such large scale vorticies whose location scales with the classical Reynolds number,

$$\mathrm{Re}_D = \frac{\rho v D}{\mu} \qquad (5)$$

where is the total fluid density and it the dynamic viscosity [20]. In the case of counterflow around a cylinder, it appears that the normal fluid, which flows upward in the channel, displays vortex shedding behind the cylinder similar to that of classical fluids. In addition, a more surprising result is the existence of a large vortex in front

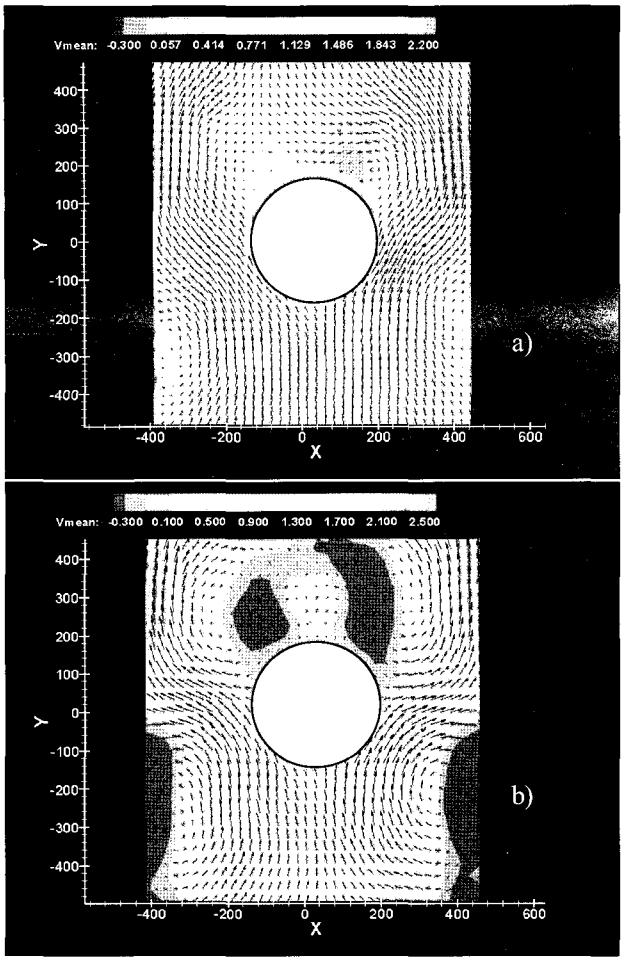

Fig. 5. Measured particle velocity field around a 6.35 mm OD cylinder. a) Heat flux is 4 kW/m2 at T = 1.6 K ReD = 41000; b) Heat flux is 11.2 kW/m2 at T = 2.03 K, ReD = 21000. The velocity scale at the top is calibrated in pixels/ms (1 pixel/ms = 22 mm/s).

of the cylinder suggesting that the superfluid component, which flows downward, may also displays this effect. One should note that the location of the large vortex in front of the cylinder is closer to the channel wall than the vortex above the cylinder. This effect may be due to the relatively stronger interaction with the normal fluid component.

By analogy to classical fluids, one might expect the observed turbulence to scale with Reynolds number, Eq. [5] with the exception that the normal fluid viscosity, μ_n, replaces the ordinary fluid viscosity, μ. However, if we compute a Reynolds number for the two examples in Fig. 5, it is immediately apparent that case a) has a Reynolds number about a factor of two larger than case b) while displaying significantly less turbulence. This suggests that the classical Reynolds number may not be the best parameter to scale turbulence in He II.

Apart from the qualitative observations of particle motion during counterflow around a cylinder and its explanation in terms of interactions with both the superfluid and normal component, we currently have no theoretical justification for these results. This is an area of current research. However, clearly the physical explanation of counterflow in other than a one dimensional channel is more complicated than previously thought. It remains to be seen how these results can help us understand the heat transport process.

5. SUMMARY

Particle Image Velocimetry is a powerful fluid dynamic tool for visualizing the entire flow field. In He II counterflow, PIV can explore the flow patterns that occur in the normal fluid component as well as that of the turbulent superfluid. In one dimensional channel counterflow, the observed flow field in steady state correlates with the normal fluid velocity although quantitatively being about half the predicted value. It is suggested that this variation may be due to an effective viscous drag by the turbulent superfluid component. Transient heat transport similarly provides qualitative agreement with the predicted velocity fields although again suggesting the existence of a superfluid drag force. For the case of counterflow around a cylinder, the PIV measurements indicate the existence of large scale vortices both in front of and behind the cylinder. Not only does this result suggest that the normal fluid component behaves similarly to a viscous fluid, but also the superfluid component shows effective viscous interactions. These findings are clearly new and subject to continued interpretation.

ACKNOWLEDGMENT

This work is supported by grants from the US Department of Energy, Division of High Energy Physics and by the National Science Foundation. The author would like to thank Drs. Tao Zhang, Sylvie Fuzier, Dogan Celik and Mr. S. Maier for their work on the experiments and analysis described in this article.

REFERENCES

[1] J.T. Tough, Superfluid turbulence, Progress in Low Temperature Physics (1982) Vol. VIII, 134-219.

[2] T. Zhang, D. Celik and S. W. Van Sciver, Tracer particles for application to PIV studies of liquid helium, *J. Low. Temp. Phys.* Vol. 134, 985 (2004).

[3] J.R. T. Seddon, M. S. Thurlow and P. G. J. Lucas, Visualizing superfluid turbulent counterflow, *J. Low Temp. Phys.* Vol. 138, 505 (2005).

[4] M. Murakami and N. Ichikawa , Flow visualization study of thermal counterflow jet in He II, *Cryogenics* Vol. 29, 438 (1989).

[5] A. Nakano and M. Murakami., Flow structure of thermal counterflow jet in He II, *Cryogenics* Vol.34 12, 991 (1994).

[6] S. W. Van Sciver, Helium Cryogenics, Plenum Press (1986).

[7] D. Landau, The theory of superfluidity of helium II *J. Phys. (U.S.S.R.)*Vol. 5, 71 (1941).

[8] S.W. Van Sciver Heat transfer through extended surfaces containing He II, *ASME Journal of Heat Transfer* Vol. 121, 142 (1999).

[9] P. Seyfert, Practical results on heat transfer to superfluid helium, Stability of Superconductors, Intern. Institute of refrigeration, p. 53 (1981).

[10] D. Celik and T Zhang., Application of PIV to counterflow in He II, Adv. Cryo. Engn. Vol. 47B, 1372 (2002).

[11] R. Donnelly, A. Karpetis, J. Niemela, K. Sreenivasan, W. Vinen, and C. White, The use of particle image velocimetry in the study of turbulence in liquid helium, *J. Low Temp. Phys.* Vol. 126, 327 (2002).
[12] D. Y. Chung and P. R. Critchlow, Motion of suspended particles in turbulent superflow of liquid helium II, *Phys. Rev. Letters* Vol. 14, 892 (1965).
[13] T. Zhang and S. W. Van Sciver, The motion of micron-size particles in He II counterflow as observed by the PIV technique, *J. Low Temp. Phys.* Vol. 138, 865 (2005).
[14] D. K. Hilton and S. W. Van Sciver, Direct measurements of quantum turbulence induced by second sound shock pulses in Helium II, *J. Low Temp. Phys.* (2005) (submitted).
[15] T. Shimazaki, M. Murakami and T. Iida, Second sound wave heat transfer, thermal boundary layer formation and boiling: highly transient heat transport phenomena in He II, *Cryogenics* Vol. 35 (10), 645 (1995).
[16] T. Zhang and S. W. Van Sciver, Use of the particle image velocimetry (PIV) technique to study propagation of second sound shock in superfluid helium, *Phys. of Fluids* Vol. 16, 99 (2004).
[17] D. Pearson and S.W. Van Sciver He II heat transfer in cylindrical geometry, Advances in Cryogenic Engineering Vol. 43, 1457 (1998).
[18] R. Maekawa, A. Iwamoto, S. Hamaguchi, and T. Mito, Subcooled He II heat transport in a channel with abrupt contractions/enlargements, Adv. Cryo. Engn. Vol. 47B, 1303 (2002).
[19] H. Tatsumoto, K. Hata, K. Hama, Y. Shirai, and M. Shiotsu, Critical heat fluxes on a flat plate pasted on one end of a rectangular duct with an orifice in pressurized He II, Adv. Cryo. Engn. Vol. 47B, 1363 (2002).
[20] H. Schlichting, Boundary Layer Theory, McGraw Hill (1979).